Talk presented at the Second LAMPF Workshop on Pion Double Charge Exchange, Los Alamos, New Mexico, August 9–11, 1989; to be published in the Proceedings by World Scientific Publishing Co.

CONF-8908131--7

PION DOUBLE CHARGE EXCHANGE SCATTERING ABOVE THE DELTA RESONANCE

George R. Burleson
Department of Physics
New Mexico State University
Las Cruces, NM 88003, U.S.A.

FG04-88ER40403

CONF-8908131--7

DE91 000606

INTRODUCTION

Talk presented at the Second LAMPF Workshop on Pion Double Charge Exchange, Los Alamos, New Mexico, August 9–11, 1989; to be published in the Proceedings by World Scientific Publishing Co.

A major program of experimental measurements of pion-nucleus double-charge-exchange (DCX) scattering began at the high-intensity accelerators a little more than ten years ago. The most extensive research has been carried out at the LAMPF accelerator in Los Alamos, New Mexico, using various beam channels and spectrometer systems. These include EPICS, for the 100-300 MeV energy range; the Low Energy Pion Channel (LEP) and the Clamshell spectrometer, for lower energies; and the P^3 Channel and the Large Aperture Spectrometer (LAS), for the higher energies, up to 550 MeV. Much theoretical study have been carried out in parallel with this work. Some of the general questions addressed include descriptions of the reaction mechanisms, the sensitivity to nuclear structure, and the relation of DCX to elastic and single-charge-exchange (SCX) scattering. The results of this work have been discussed extensively at two workshops held at LAMPF, one in 1985,[1] and a very recent one in August,

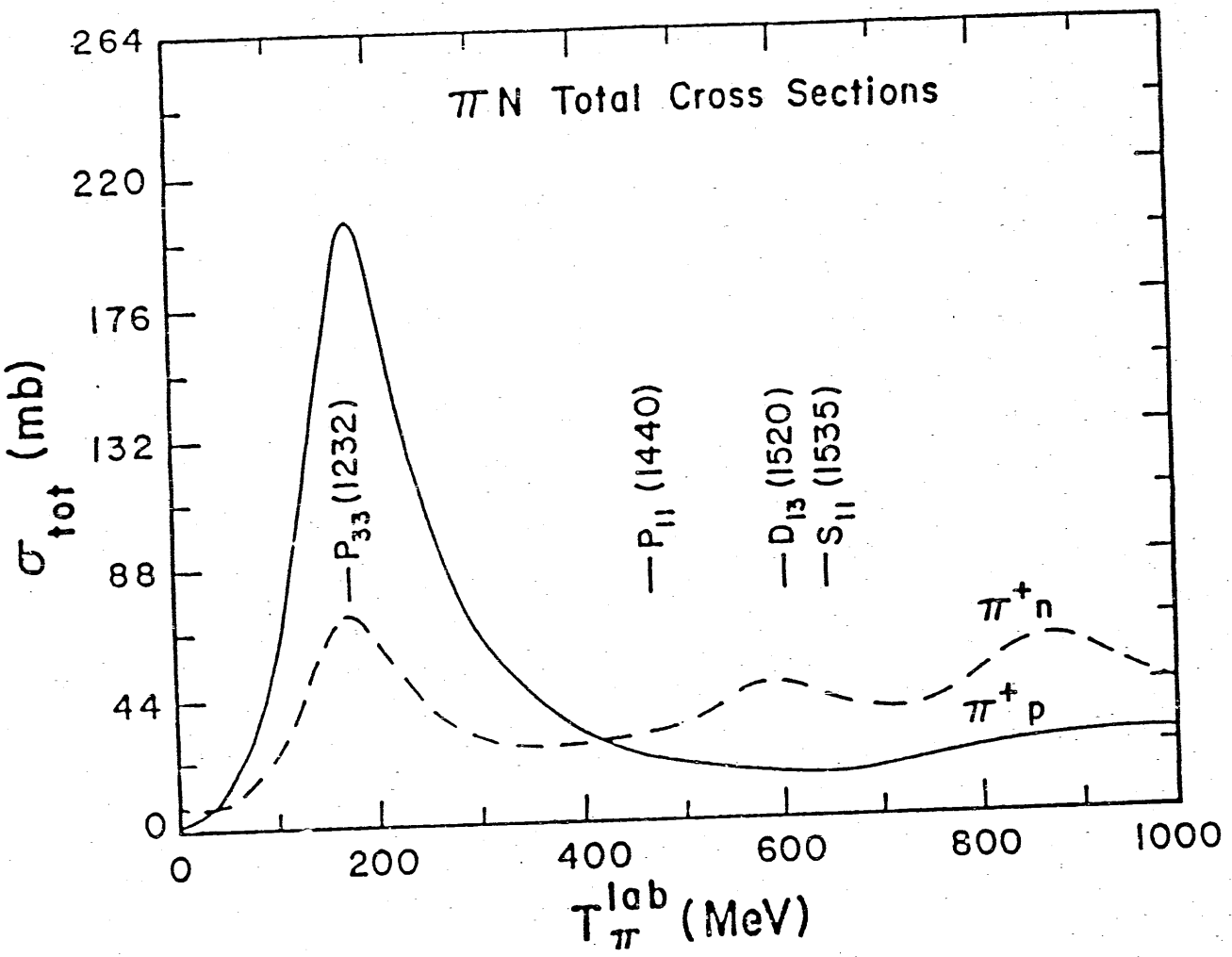

FIG. 1. Pion-nucleon total cross sections as a function of energy. The solid line represents $\pi^+ p$ ($\pi^- n$) and the dashed line represents $\pi^+ n$ ($\pi^- p$). The energies where pion-nucleon resonances are found are indicated.

causing the π^+:π^- ratio to be about 1:1 rather than the well-known 9:1 value found in the Δ region. The collision length at 500 MeV is $\sim$ 3 fm, as contrasted with $\sim$ 0.3 fm at 180 MeV, near the peak of the Δ resonance. This causes the pion to penetrate further into the nucleus, though not into the deep interior. Such a penetration may give greater sensitivity to nucleon-nucleon correlation effects than at the Δ resonance, since the pion can interact with more nucleons.

Another simplification arises from the expected higher rate of convergence of perturbation theory. The ratio of the second-order optical potential to the first-order term has been estimated by Ernst, et al,[1,2] to be given by $R = \rho \ell_c \sqrt{\sigma}/k$, where ρ is the nuclear density, ℓ_c the correlation length, σ the total cross section, and k the pion wave number. Estimates[1] of R which use nuclear densities in the pion interaction region and take ℓ_c to be 1 fm give $\sim$ 0.1 at 160 MeV and $\sim$ 0.04 at 500 MeV, which indicate that the multiple scattering series should be more convergent at the higher energies. A test of this is a comparison of elastic scattering data with theory that might be based, for example, on a good first-order optical potential. It should be possible to make such a comparison fairly soon, since a representative set of $\pi^\pm$ elastic scattering cross sections at these energies have been measured and are currently being analyzed.[3]

Another characteristic of this region is a fairly flat energy dependence of the forward-angle pion-nucleon single-charge-exchange cross section (SCX), which should help simplify calculations of double-charge-exchange scattering (DCX) at small angles. In addition, pion absorption should be a smaller complication, since at 300 MeV it is dropping faster than is the total pion-nucleus cross section.[4] We also note that at these energies the Q-values for DCX reactions are small with respect to the beam energies, as contrasted with the situation at low energies, which is a possible complication in the interpretation of some of the low-energy results.[5]

All of this indicates that a great deal of simplicity in the pion-nucleus interaction is found in this energy region and that theoretical calculations here should in principle be more reliable than at lower energies.

THE EXPERIMENTAL DATA

The data I will present were all taken on the P^3 Channel at LAMPF, which was modified two years ago, along with the Large Aperture Spectrometer (LAS) used there, to give improved resolution.

A new tune of the channel was developed, which gives a dispersed beam spot (as at the EPICS system at LAMPF), 2 cm per percent $\Delta p/p$, with a size of about 6 x 6 cm. The flux under these conditions is about 2 x 10^7 π^+/s at 450 MeV. The spectrometer was instrumented with new drift chambers to improve spatial resolution and with a gas threshold Cherenkov counter to reject electrons,

and a sweeping magnet was installed near the target to separate pions of opposite charge. The spectrometer solid angle is $\sim$ 12 msr, its angular acceptance is $\pm 4^0$, its angular resolution is $\sim 1/2^0$, its momentum acceptance is $\pm 10\%$, and its energy resolution is $\sim$ 2 MeV at 500 MeV.

The experimental runs took place over a three-year interval, 1987-89, with slightly different experimental conditions each year. The collaboration includes physicists from Texas, LAMPF, New Mexico State, Pennsylvania, and Colorado.[1] Some of the results I will present here have been published,[6] but most of them are new, in that they have not been published and have not been presented at any conference. The unpublished results should be considered preliminary.

Analog Transitions: General Characteristics

An example of the spectra measured at 5^0 is shown in Fig. 2. For ^{14}C, the analog peak is separated by 5.2 MeV from the first excited state, so that we have a clean determination of the yield. For ^{18}O, contributions from the 2^+ state at 1.89 MeV and the $(0^+, 2^+, 4^+)$ triplet at $\sim$ 3.5 MeV cannot be resolved from the ground-state (analog) peak, but their contrtibutions are expected to be small at small angles. These spectra are from the first year of data-taking, when the resolution was poorer than it was later.

Differential cross sections for various nuclei at small angles as a function of energy are shown in Fig. 3. The agreement of the new data points with previously measured ones[7] is very good. These data show the energy exciteation functions to be fairly flat, as might be expected from the flatness of the pion-nucleon cross sections. We note that the 0^0 SCX cross sections on several nuclei at these energies were found to increase with energy fairly markedly here,[8] contrary to the behavior of the free pion-nucleon charge-exchange cross section, which is fairly flat.

An example of the SCX data is presented in Fig. 4, compared with our data on ^{14}C and ^{18}O, together with data at lower energies.[7] Calculations of Parnell and Ernst[9] for both SCX and DCX are also shown. The agreement of these calculations with the SCX data at higher energies is fairly good, but the predicted DCX cross sections are below the data by a factor of about three. These calculations are based on a first-order optical potential with no free parameters, in which the transition to the double isobaric analog state (DIAS) proceeds by sequential scattering through the single isobaric analog state (IAS). They contain s, p, and d pion-nucleon partial waves, but pion absorption is not included. A prediction of the six-quark bag model of Miller[10] is also shown in Fig. 4, which indicates a

[1]The participants are A. Williams, K. Johnson, G. Kharimanis, C. Fred Moore, S. Mordechai, and H. Ward, University of Texas; L. Agnew, L. Atencio, H. Baer, J. McGill, C. Morris, and S. Schilling, LAMPF; G. Burleson, K. Dhuga, J. Faucett, G. Kyle, and M. Rawool, NMSU; M. Burlein, H. T. Fortune, E. Insko, R. Ivie, J. O'Donnell, J. Silk, D. Smith, and J. Zumbro, University of Pennsylvania; and D. Oakley, University of Colorado.

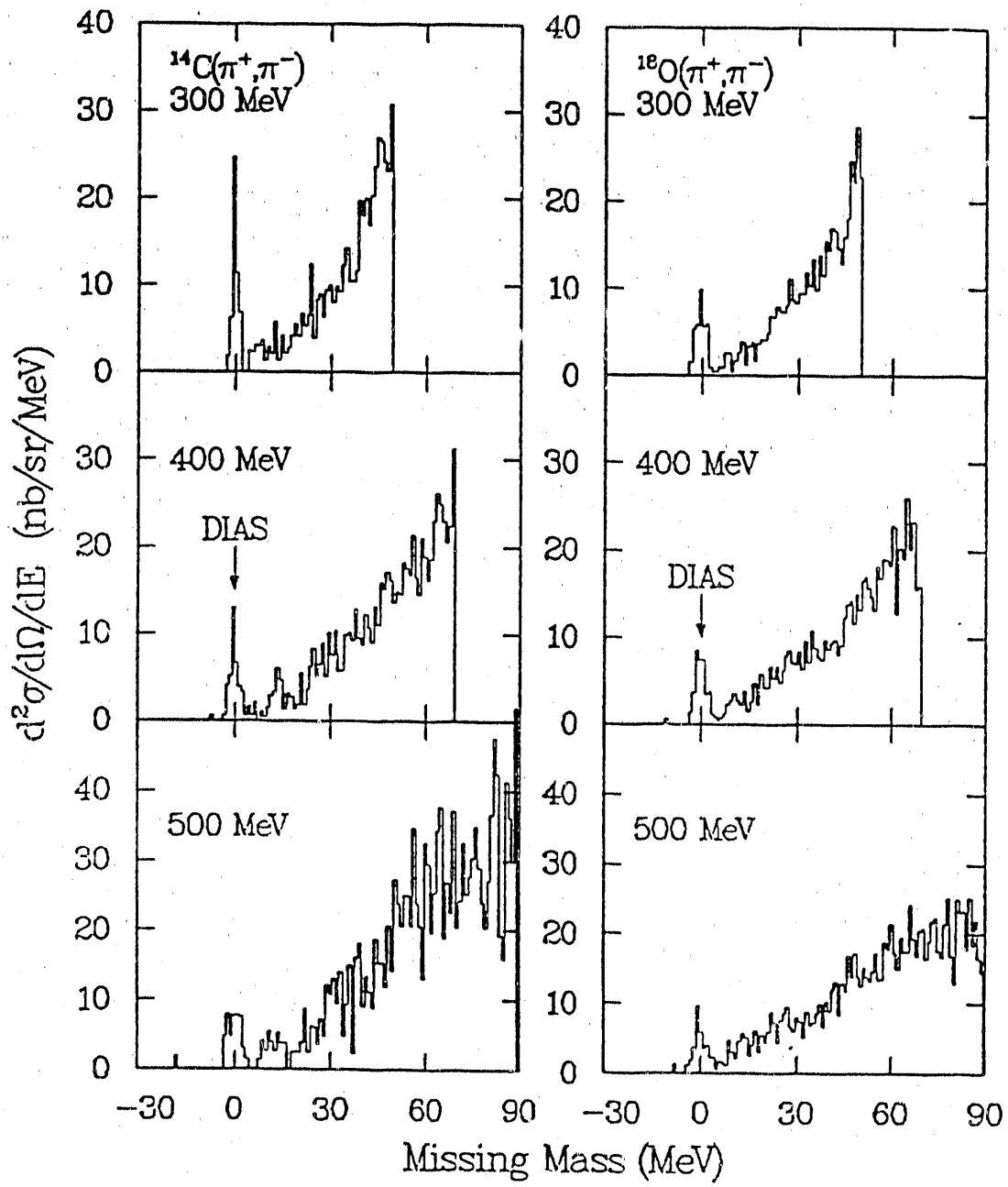

FIG. 2. Spectra for the (π^+,π^-) reaction on ^{14}C and ^{18}O measured with the Large Acceptance Spectrometer (LAS) at the P^3 channel at LAMPF at a 5^0 laboratory angle, corrected for the acceptance of the spectrometer.

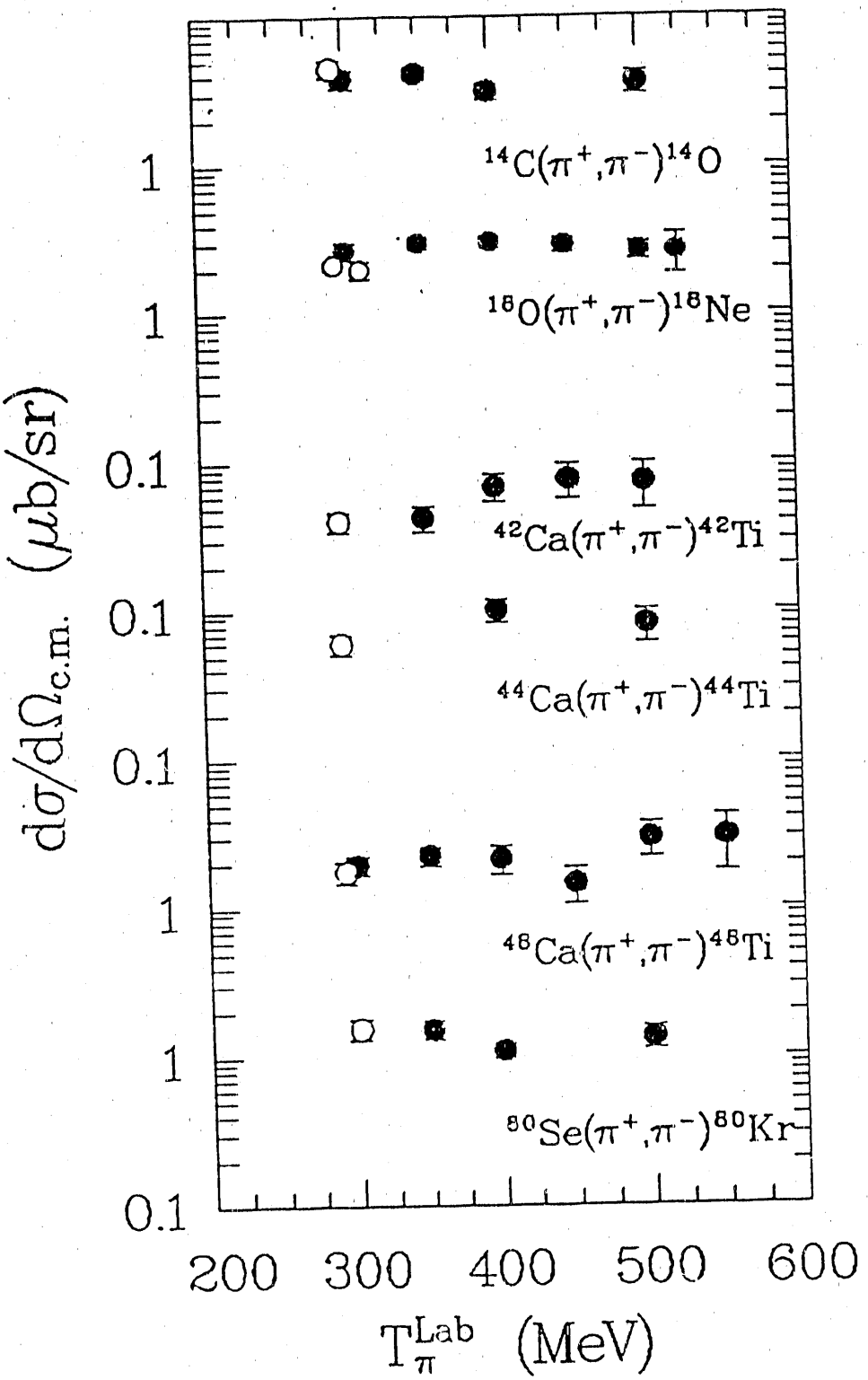

FIG. 3. Small-angle differential cross sections for the (π^+,π^-) reactions to the double isobaric analog state on the nuclei indicated. The filled circles represent data from the work reported here and the open circles represent previous data.[7]

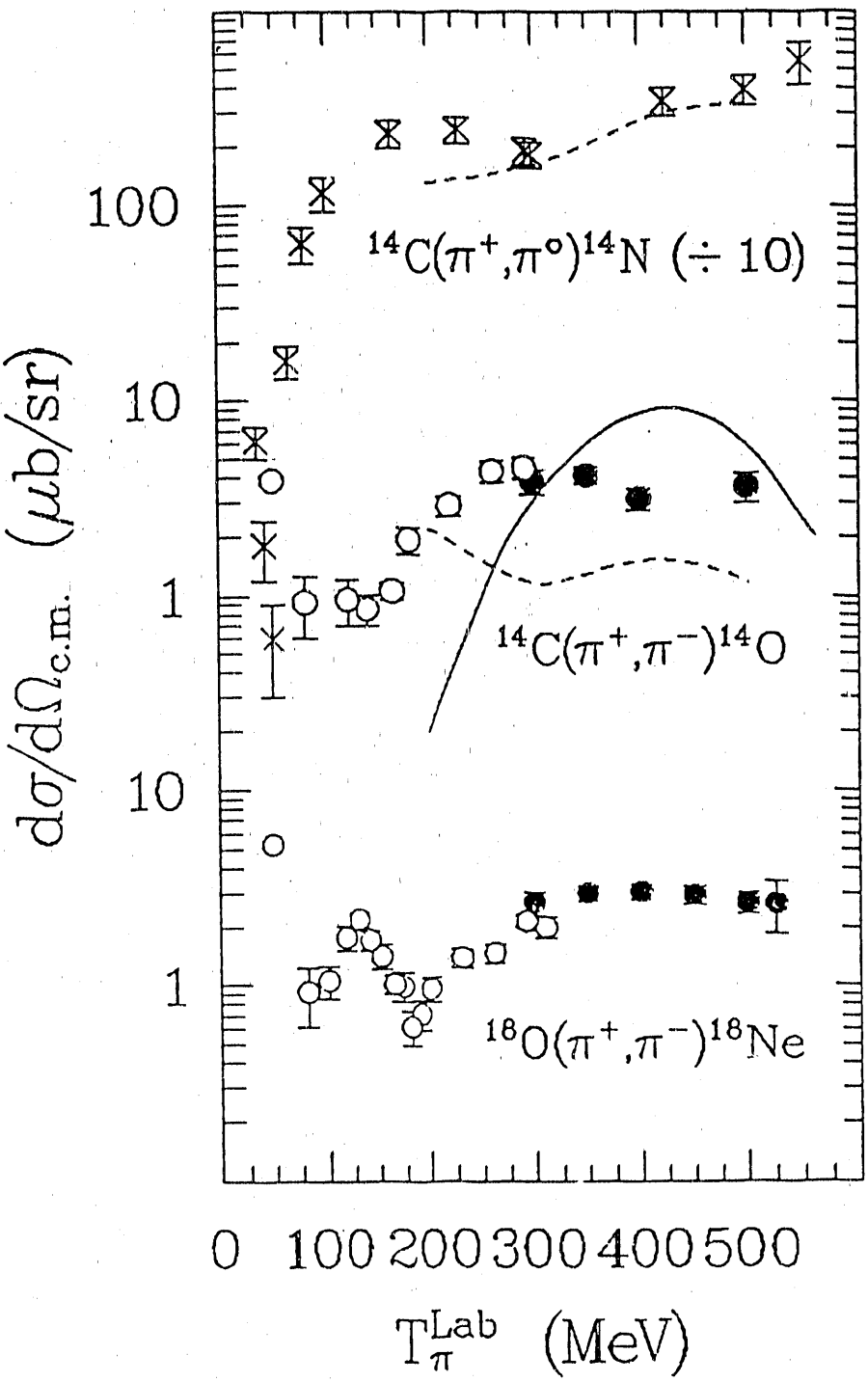

FIG. 4. The 0^0 cross sections as a function of energy for SCX transitions to analog states from ^{14}C (top, crosses), and the 5^0 cross sections for DCX transitions to analog states from ^{14}C and ^{18}O. The filled circles are from the work reported here and the open circles represent previous work. The theoretical curves are from Ref. 10 (solid curve) and Ref. 9 (dashed curve).

resonance-like behavior. The data show no such behavior, so that no signature of such a six-quark bag is seen in DCX in this energy region.

The A-dependence of the cross sections is usually displayed as plots of the cross section $d\sigma/d\Omega$ divided by $(N-Z)(N-Z-1)$, which represents the product of the numbers of neutrons available for sequential SCX processes. As might be expected from the results shown in Fig. 3, such plots of our data at 400 and 500 MeV are very similar. The one I feel is most enlightening to show is Fig. 5, at 500 MeV, but which also contains our 450-MeV data on several $f_{7/2}$-shell nuclei, discussed below. The lines shown represent an $A^{-7/3}$ dependence, which seems to be a fair representation of the general trend of the data. For comparison, the DIAS data between 100 and 300 MeV were all found to be consistent with an $A^{-10/3}$ dependence, and the isospin-one data alone were found to have a best-fit exponent of -7/3.[11] The results here suggest a weakening of the DCX interaction at energies above 300 MeV, as might be expected from the smaller total cross sections.

We also have data on one angular distribution, for ^{18}O at 400 MeV, shown in Fig. 6. At the larger angles we expect contributions to the analog peak from the higher states mentioned above, as is suggested by the shift in the centroid of the peak shown in the inset in Fig. 6. We estimated cross sections to the DIAS alone by fitting two peaks to the spectra, with results also shown in that figure. There are no published calculations for DIAS angular distributions at these energies to compare with these results, however.

Analog Transitions: Data on $f_{7/2}$-Shell Nuclei

The data on $f_{7/2}$-shell nuclei mentioned above were taken partly to compare with the two-amplitude model[12,13] discussed in the previous two talks. I remind you that this model describes the DCX process for nuclei which have excess neutrons within a single shell in terms of two amplitudes, generally called A and B. The A amplitude corresponds to transitions through analog states and involve long-range effects without nucleon correlations, whereas the B amplitude arises from short-range correlations and represents transitions through, or to, nonanalog states. This model was introduced partly to explain the observed ratios of DCX cross sections on the calcium isotopes, which did not follow the behavior expected from the It can predict not only analog transitions but transitions to nonanalog ground states as well. With a simplified version of the shell model known as the seniority scheme, the forms of these predictions are fairly simple, as shown in Table I. For more realistic calculations, corrections are needed which correspond to more realistic shell-model wave functions and to accounting for distortion effects.

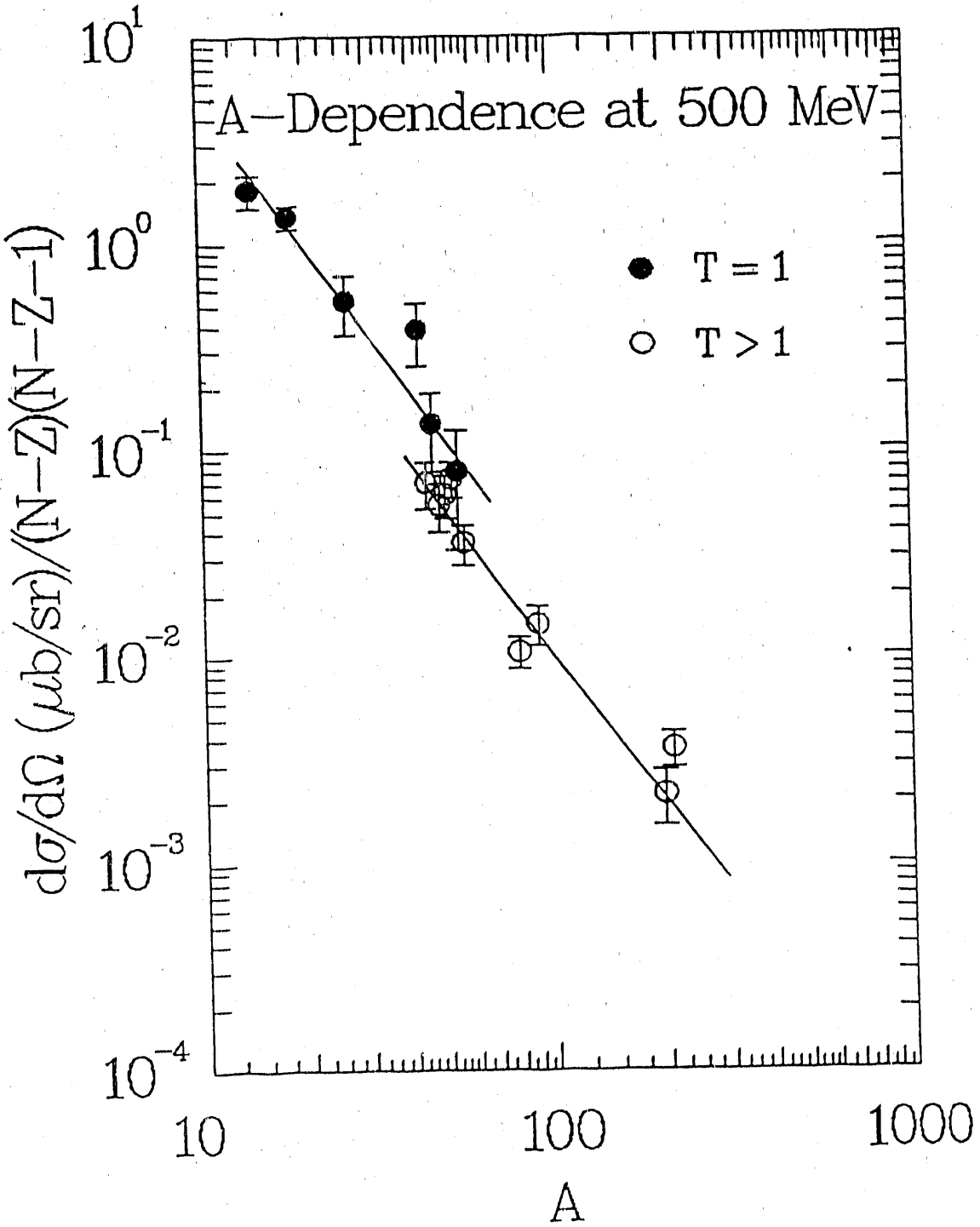

FIG. 5. Small-angle differential cross sections at 500 MeV for the DCX reaction to analog states, divided by $(N-Z)(N-Z-1)$, as a function of nuclear number A. Some 450-MeV data points for nuclei with A between 42 and 54 are also included. The filled circles represent T = 1 nuclei and The open circles represent T > 1 nuclei. The curves represent an $A^{-7/3}$ dependence.

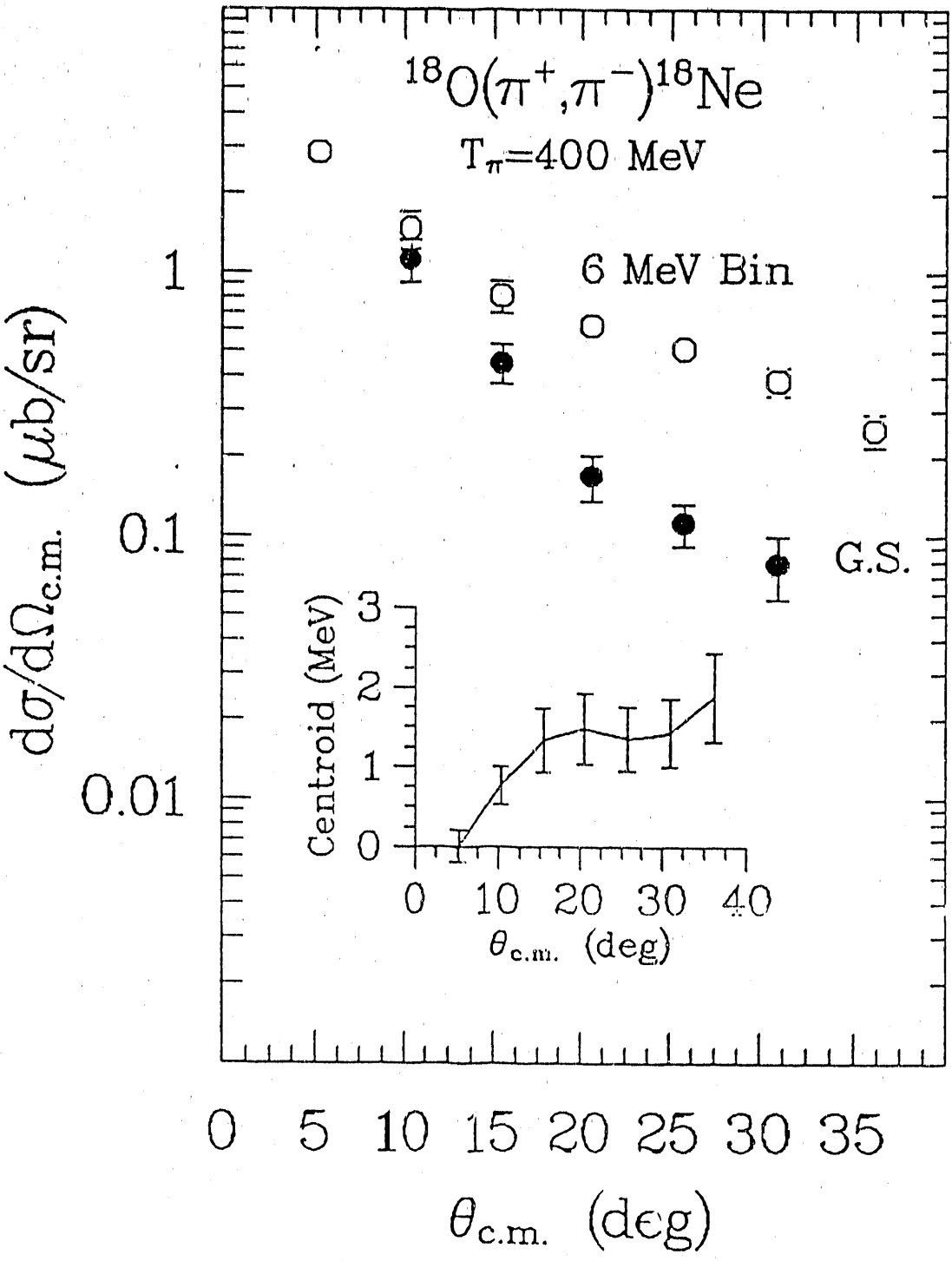

FIG. 6. The measured angular distribution for the $^{18}O(\pi^+,\pi^-)^{18}Ne$ (0-6 MeV) reaction, shown by open circles. The filled circles represent the estimated cross sections for the ground state. The inset figure shows the change in the centroid of the 0-6 MeV bin as a function of angle.

TABLE I

DCX Cross Sections for $f_{7/2}$-Shell Nuclei in the Seniority Model, from the Two-Amplitude Model of Refs. 12-13

Isospin	Nuclei	$d\sigma/d\Omega$(DIAS)	$d\sigma/d\Omega$(g.s.)
1	^{42}Ca,^{54}Fe	$\|A + B\|^2$	-
2	^{44}Ca,^{52}Cr	$6\|A + 0.11B\|^2$	$1.58\|B\|^2$
3	^{46}Ca,^{50}Ti	$15\|A - 0.07B\|^2$	$1.94\|B\|^2$
4	^{48}Ca	$28\|A - 0.14B\|^2$	$1.36\|B\|^2$
1	^{46}Ti,^{50}Cr	$\|A + 1.47B\|^2$	-
2	^{48}Ti	$6\|A + 0.17B\|^2$	$2.3\|B\|^2$

We have two sets of measurements to compare with this model. As shown in Fig. 3, we have data on ^{42,44,48}Ca at 5^0 between 300 and 500 MeV, and we also have 5^0 data at 450 on ^{46,50}Ti, ^{52}Cr, and ^{54}Fe. We have fitted these data to this model, using correction factors for shell-model and distortion effects given us by Gibbs,[14] for all results reported here. The correction factors lie generally in the range of 0.4–0.9, but for distortions they include pion-nucleon s- and p-waves only. The fitted values of the parameters depend on these corrections, of course, but the general conclusions below do not depend on whether or not the corrections are used.

I will first discuss our fits to the calcium isotope data. One difficulty we have is that the experimental ground-state cross sections are very small; in some cases we only have upper limits. All our attempts to fit these data at any energy to the formulas in Table I, with or without corrections, have met with failure, because the ground-state cross sections are too low. Without the ground states, of course, all one can do is to find values of A, B, and cos ϕ, where ϕ is the phase angle between A and B, with their errors, since we use only three cross sections as inputs. Some of the results of such a fit are shown in Fig. 7, which presents the ratio $|B|/|A|$ as a function of energy, based on fits to the analog states of the calcium isotopes only. (We include some results from fits to data at lower energies as well.) The curve shown is a calculation of this ratio given us by Gibbs,[14] based on Ref. 13, again using only pion-nucleon s- and p-waves. It indicates an increase with energy that is consistent with the fitted results. This increasing ratio is puzzling, because the constancy of the cross sections indicate that A should be rather flat, since is it weighted more heavily in the formulas, and that B should be rising (both of which we find in the fits). But the ground-state strength is proportional to $|B|^2$, so that the ground-state cross sections should be increasing as well, contrary to what we find. To emphasize the extent of the discrepancy between the ground-state cross sections predicted by these fits and the experimental values, I have combined all data in the 400-500 MeV range and fitted the analog states only. For ^{44}Ca the predicted ground-state cross section is 0.35 μb/sr (with the Gibbs corrections), whereas the averaged experimental

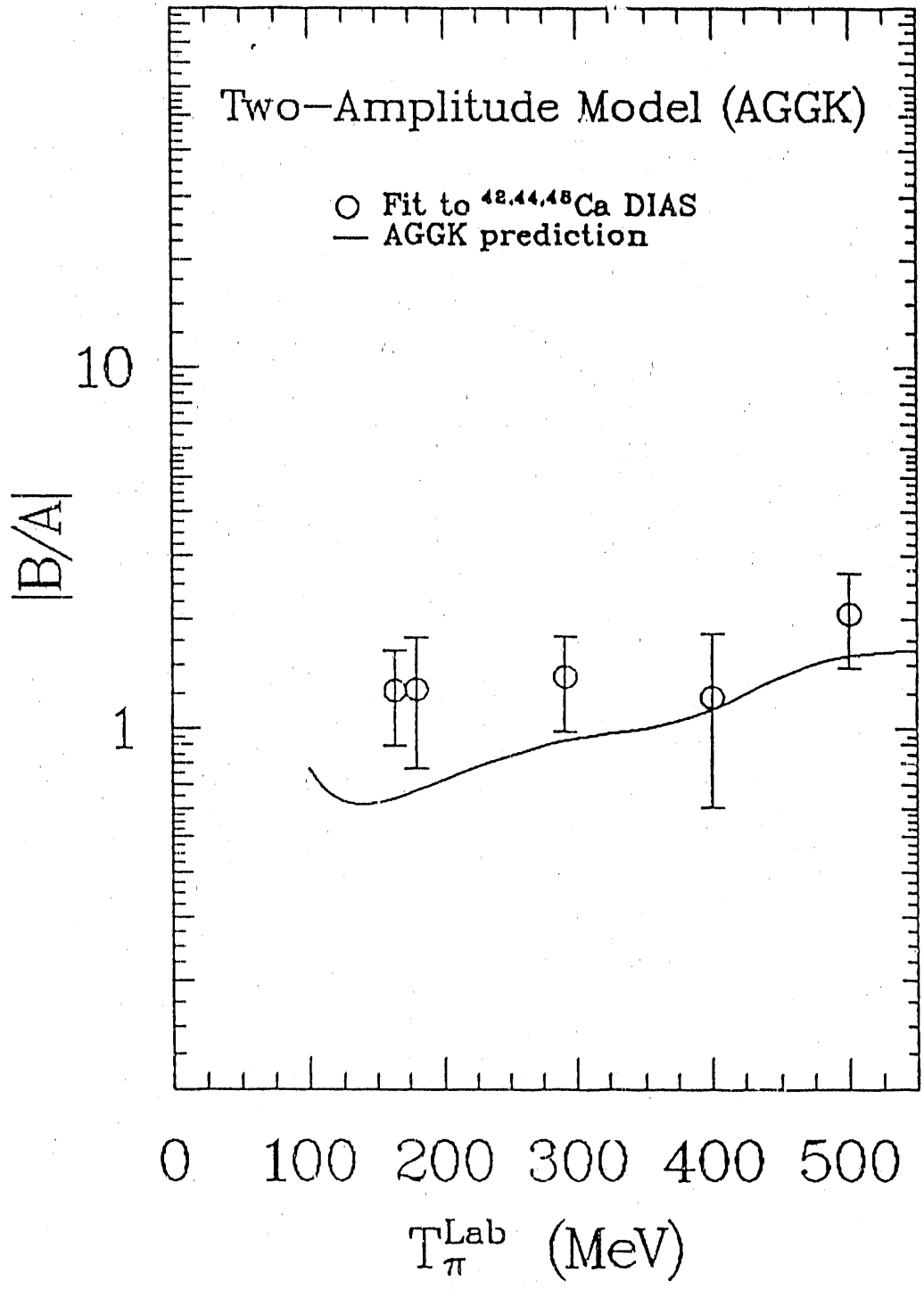

FIG. 7. Values of the amplitude ratio |B|/|A| as a function of energy, from fits of the model of Ref. 13 to forward-angle differential cross sections for DCX transitions in ^{42,44,48}Ca to analog states. The curve is a prediction of Gibbs for this ratio, based on Ref. 13.

value is 0.076 ± 0.040 μb/sr, and for ^{48}Ca the prediction is 0.38 μb/sr, compared with the experimental value of 0.035 ± 0.035 μb/sr. The differences are about 7 and 10 standard deviations, respectively! (Please keep in mind, however, that I am quoting preliminary results.) The experimental ground-state cross sections compared with predictions of fits to the analog states are shown in Figs. 8 and 9. Again, we show results from lower-energy data as well, for comparison.

To study this model further, we measured cross sections on four other $f_{7/2}$-shell nuclei at 450 MeV, 5^0. To see how well they agree with the previous fits, we used the combined 400-500 MeV data for the calcium isotopes. (For ^{44}Ca this is necessary, since we have no data at 450 MeV.) Again we find the ground-state problem, which I will discuss below, but we find another problem as well. As can be seen in Table I, the nuclei that carry the most weight for the B amplitude in these fits are those with T = 1. For this study, we have three such nuclei, ^{42}Ca, ^{46}Ti, and ^{54}Fe, with ^{42}Ca being the"standard" one used in nearly all studies so far. With these data, however, we find that if we restrict ourselves to analog states only, we cannot fit both ^{42}Ca and the (^{46}Ti, ^{54}Fe) pair, together with the remainder of the data. Some examples of fits we have tried are shown in Table II. Without ^{46}Ti and ^{54}Fe, the fitted values are similar to the ones we found with the calcium isotopes only, which shows that ^{50}Ti and ^{52}Cr are consistent with predictions from the calcium fits. The measured cross sections for ^{46}Ti and ^{54}Fe, however, are 3 to 4 standard deviations away from the values predicted by this fit, as shown in Fig. 10. On the other hand, if we take all the data, but without ^{42}Ca, or even without any of the calcium isotopes, we also find satisfactory fits, in the sense of having good χ^2 values, but we find that cos ϕ is essentially undetermined, as contrasted with what we find with good fits which include the calcuim isotopes. Without the calcium isotopes, however, B is considerably smaller than A.

TABLE II

Fits of the DIAS Cross Section of the $f_{7/2}$-Shell Nuclei at 450 MeV to the Two-Amplitude Model

Nuclei Fitted	Reduced χ^2	|B|/|A|	cos ϕ
^{42,44,48}Ca only	0	1.62 ± 0.38	0.56 ± 0.32
Without ^{46}Ti,^{54}Fe	1.6	1.36 ± 0.36	0.74 ± 0.36
All	3.2	0.81 ± 0.11	1.00 ± 0.37
Without ^{42}Ca	1.7	0.59 ± 0.16	1.0 ± 1.2
Without ^{42,44,48}Ca	0.7	0.29 ± 0.17	1.0 ± 2.0

As mentioned above, the ground-state problem is still present, as can be seen in Fig. 11, which shows the experimental ground-state cross sections compared with the prediction of the fit to the set of analog states without ^{46}Ti and ^{54}Fe. The indication of all this seems to be that the model certainly seems to have some validity, but that it needs further study.

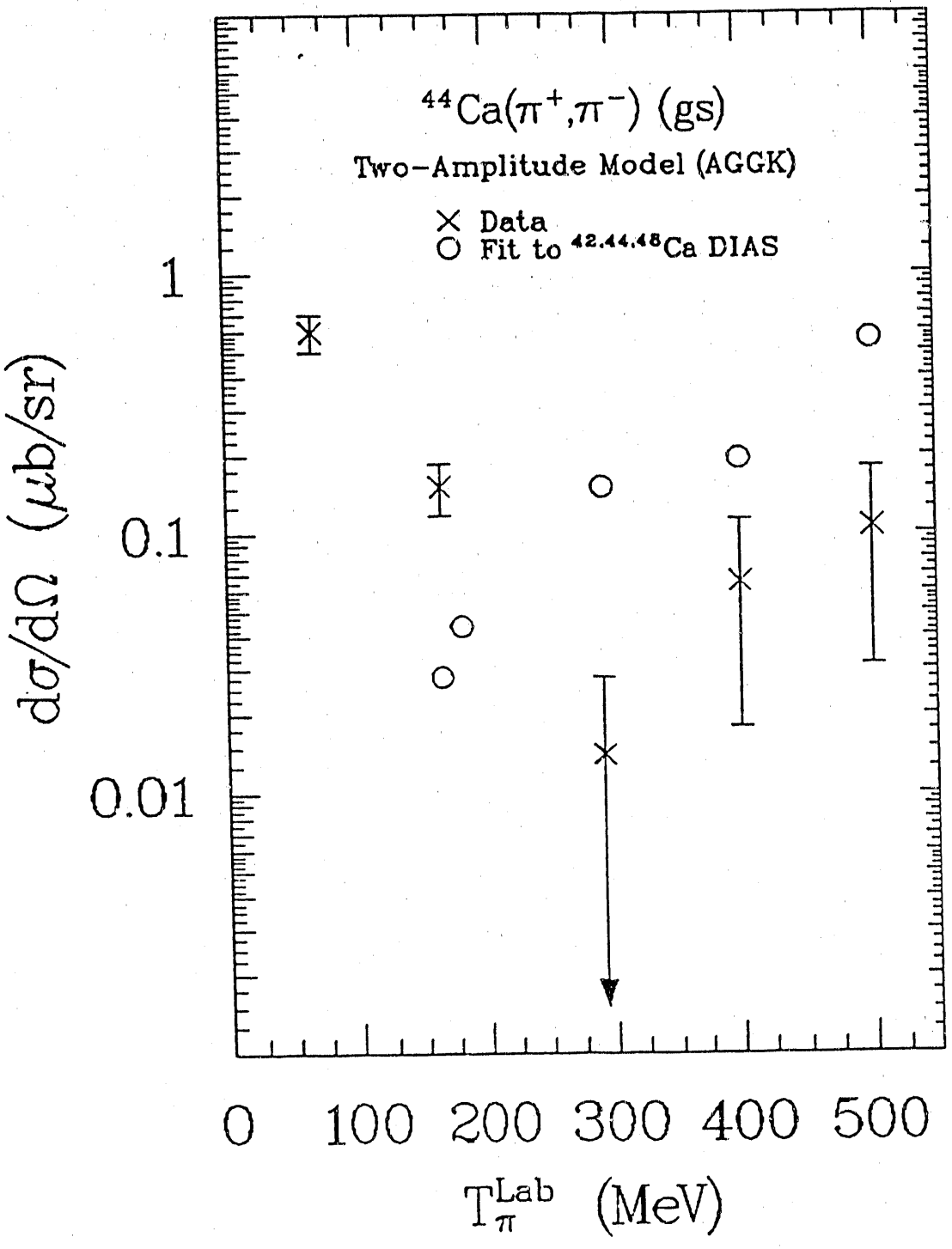

FIG. 8. Predictions of ground-state cross sections for DCX transitions in ^{44}Ca as a function of energy, from fits to DCX analog transitions in ^{42,44,48}Ca (open circles) of the model of Ref. 13. The experimental values of these cross sections are shown by the crosses.

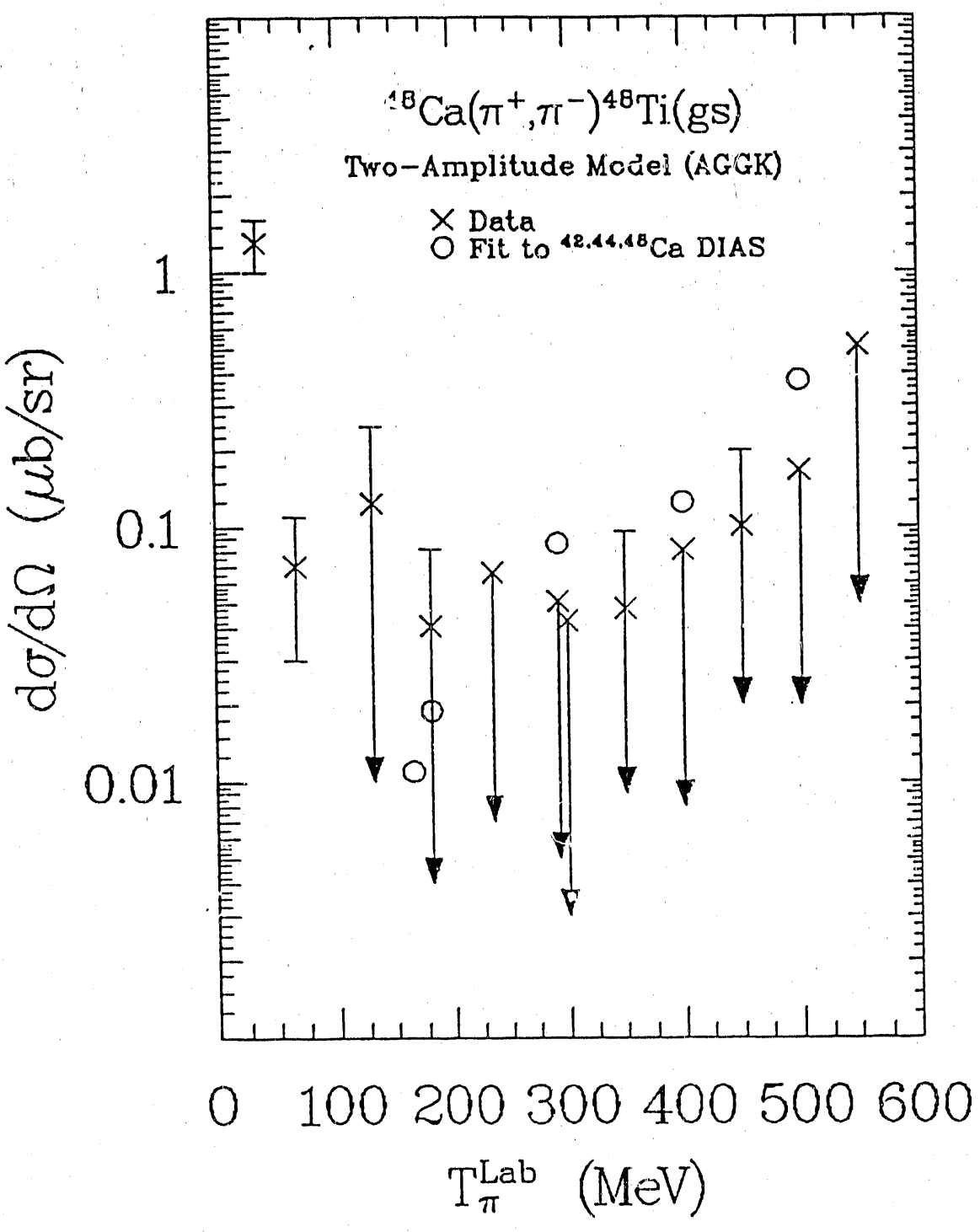

FIG. 9. Predictions of ground-state cross sections for DCX transitions in ^{48}Ca as a function of energy, from fits to DCX analog transitions in $^{42,44,48}Ca$ (open circles) of the model of Ref. 13. The experimental values of these cross sections are shown by the crosses.

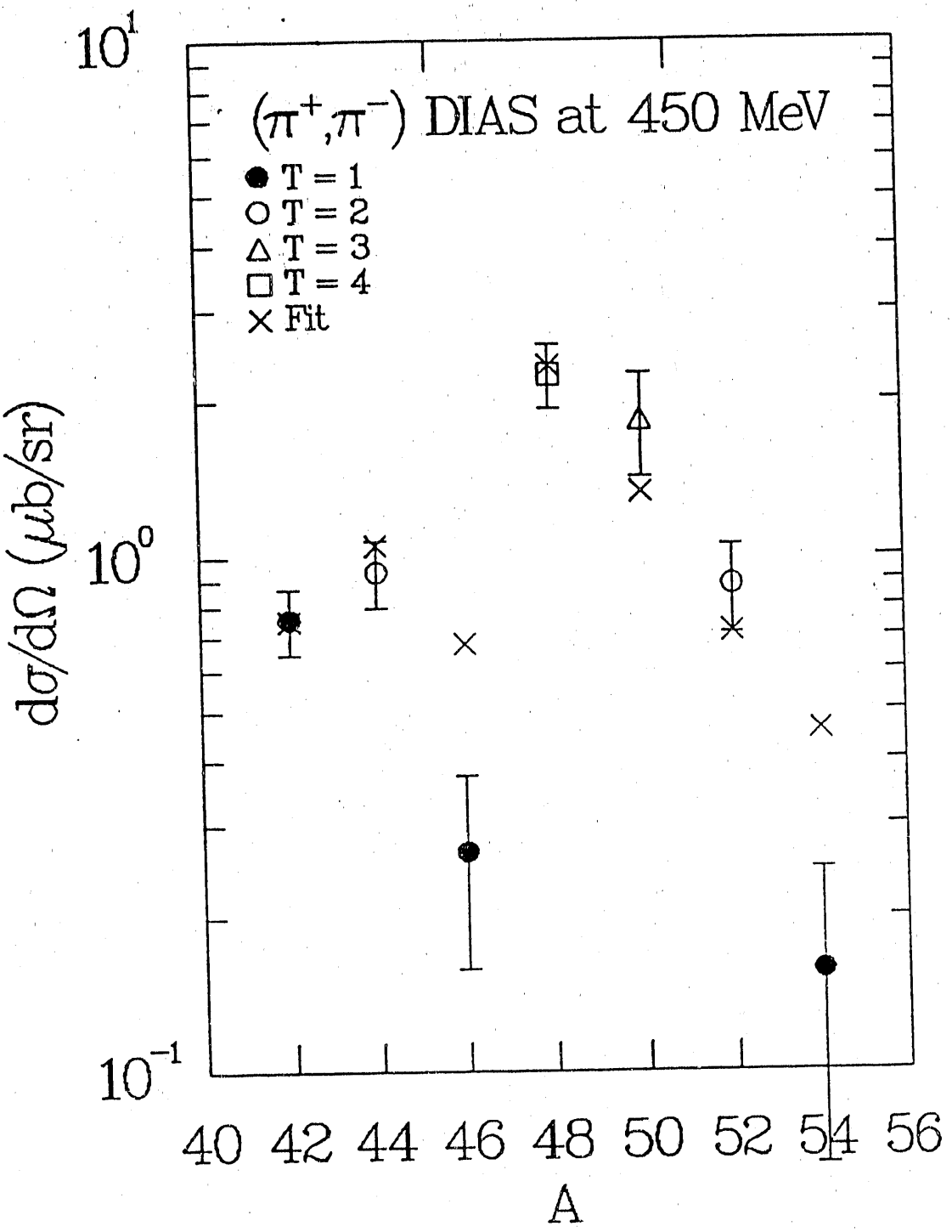

FIG. 10. Results of a fit of cross sections for DCX analog transitions in the $f_{7/2}$-shell nuclei ^{42,44,48}Ca, ^{50}Ti, and ^{52}Cr at 450 MeV to the model of Ref. 13, as a function of nuclear number A (crosses). Also shown are predictions of cross sections for ^{46}Ti and ^{54}Fe (crosses). The experimental data are shown with the symbols indicated for different values of the isospin T.

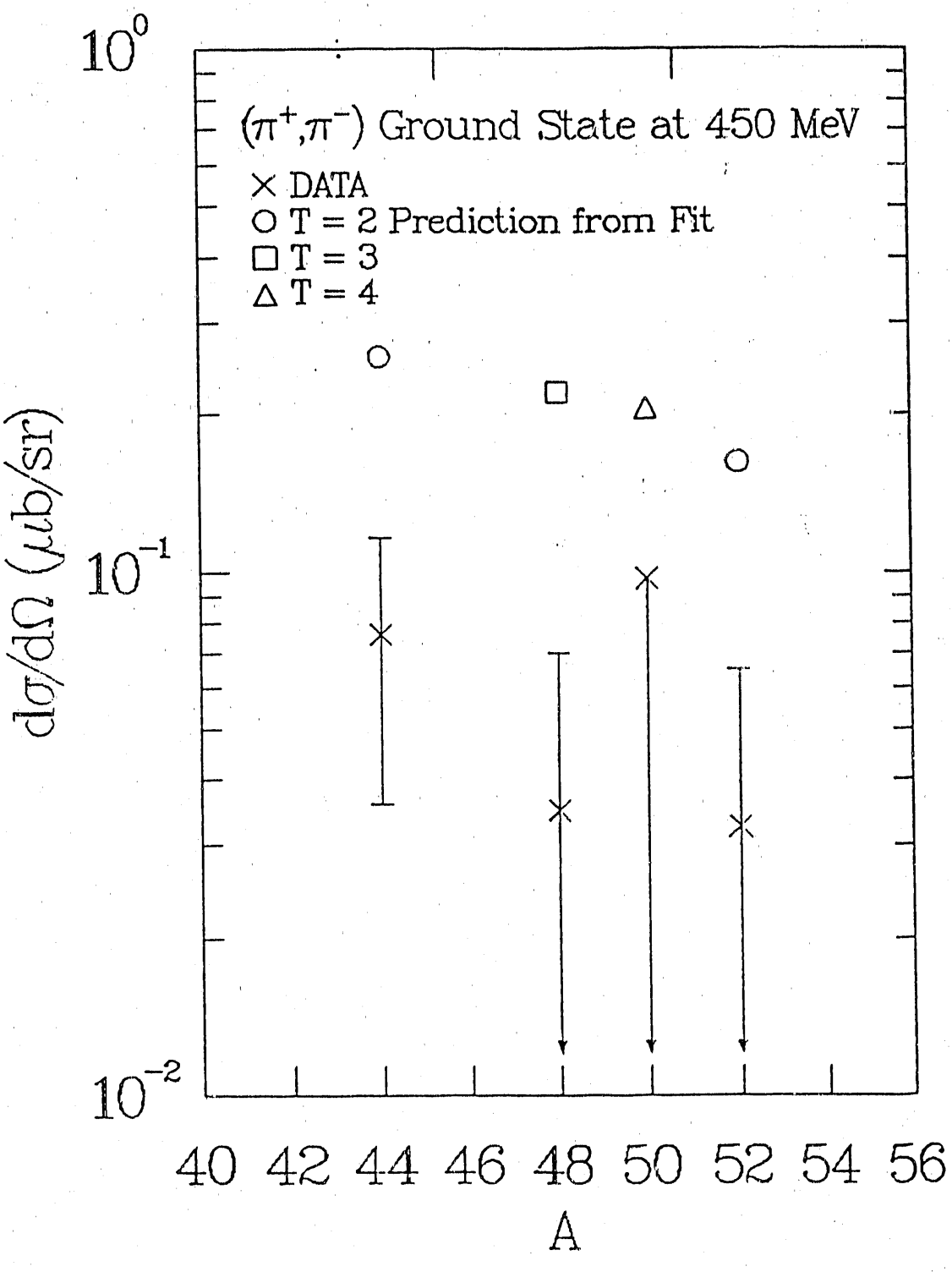

FIG. 11. Predictions of the fit of Fig. 10 for DCX transitions to the ground states of $f_{7/2}$-shell nuclei, as a function of nuclear number A, shown with the symbols indicated for different values of the isospin T. The experimental data are also shown, indicated by crosses.

Nonanalog Data

The only nonanalog excitation function we have measured is for the $^{16}O(\pi^+,\pi^-)^{16}Ne$ reaction, shown in Fig. 12 along with data from lower energies. Again, the data appear to indicate a flat behavior between 300 and 500 MeV. There are no published calculations of nonanalog transitions in this region to compare these results with, however. We have little more information beyond this as yet, since we have not measured cross sections on enough other nuclei to find a meaningful A-dependence, and we have measured no angular distributions.

We have found a rather unexpected feature in nonanalog transitions in the continuum region, however, which is illustrated in Figs. 13 and 14. Fig. 13 shows our spectra on ^{16}O and ^{48}Ca at different energies. The striking feature of the ^{48}Ca spectra is a strong tendency of the nonanalog background around the analog peak to drop with increasing energy. (It is really this behavior that makes many of these measurements possible!) We have also seen this effect with ^{208}Pb in a comparison of our 500-MeV data with previous data at 295 MeV.[15] To express this effect quantitatively, we have integrated the nonanalog portions of the ^{48}Ca spectra from threshold up to 18 MeV of excitation, with the results shown in Fig. 14. For comparison purposes, we have done the same with the ^{16}O spectra, which are also shown in Fig. 14. The ^{16}O spectra themselves are shown in Fig. 13. I should note that the ground-state peaks do not appear prominent here because these data were taken during the first year when the resolution was poorer, and because we had to use a very thick target; with a larger vertical scale, the peaks would be more easily seen. The falling trend with these data is seen in ^{16}O and possibly in ^{48}Ca. The 450-MeV point with ^{48}Ca is out of line with this general trend; we are not sure now whether this is a real effect or not, but we hope to study it further. We also expect to take additional data in the near future, to address a number of other questions that have been raised by these results.

SUMMARY

The energy region around 300-500 MeV is very attractive for pion-nucleus studies. Pion-nucleon total cross sections are fairly flat and are not dominated by resonances. The penetration of the pion into the nucleus is greater than at the $\Delta(1232)$ resonance. Pion absorption also appears to be smaller. The expansion parameter for multiple scattering here should be smaller than at lower energies, so that theoretical calculations here should be more reliable. This can be tested with elastic scattering data, which should soon be available.

Experimental cross sections for analog transitions at small angles with a range of nuclei indicate that the excitation functions at these energies are fairly flat, and that the A-dependence, divided by $(N-Z)(N-Z-1)$, can be represented

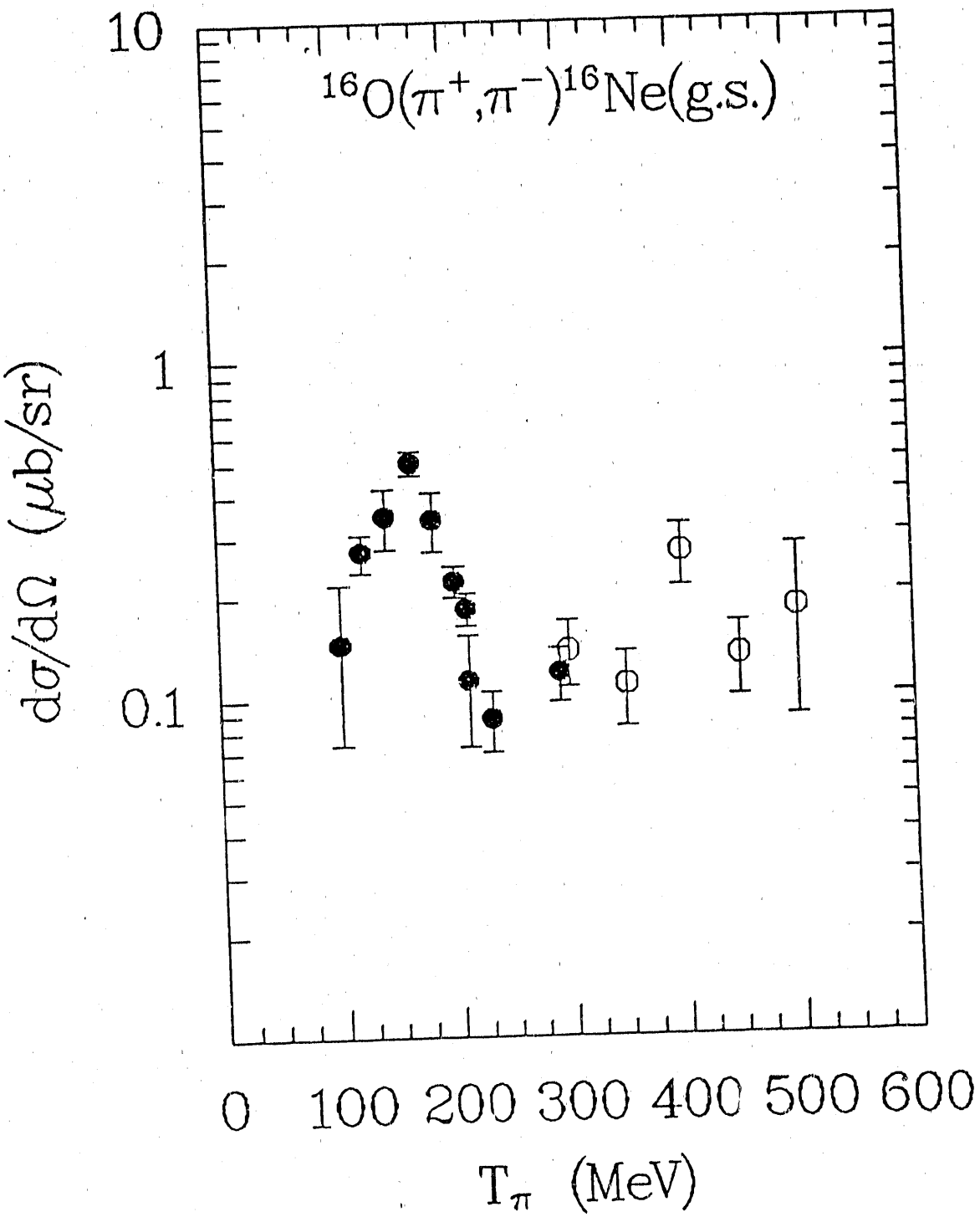

FIG. 12. Small-angle differential cross sections for the $^{16}O(\pi^+,\pi^-)^{16}Ne$ reaction to the ground state as a function of laboratory energy. The open circles represent data from the work reported here and the filled circles represent previous data.

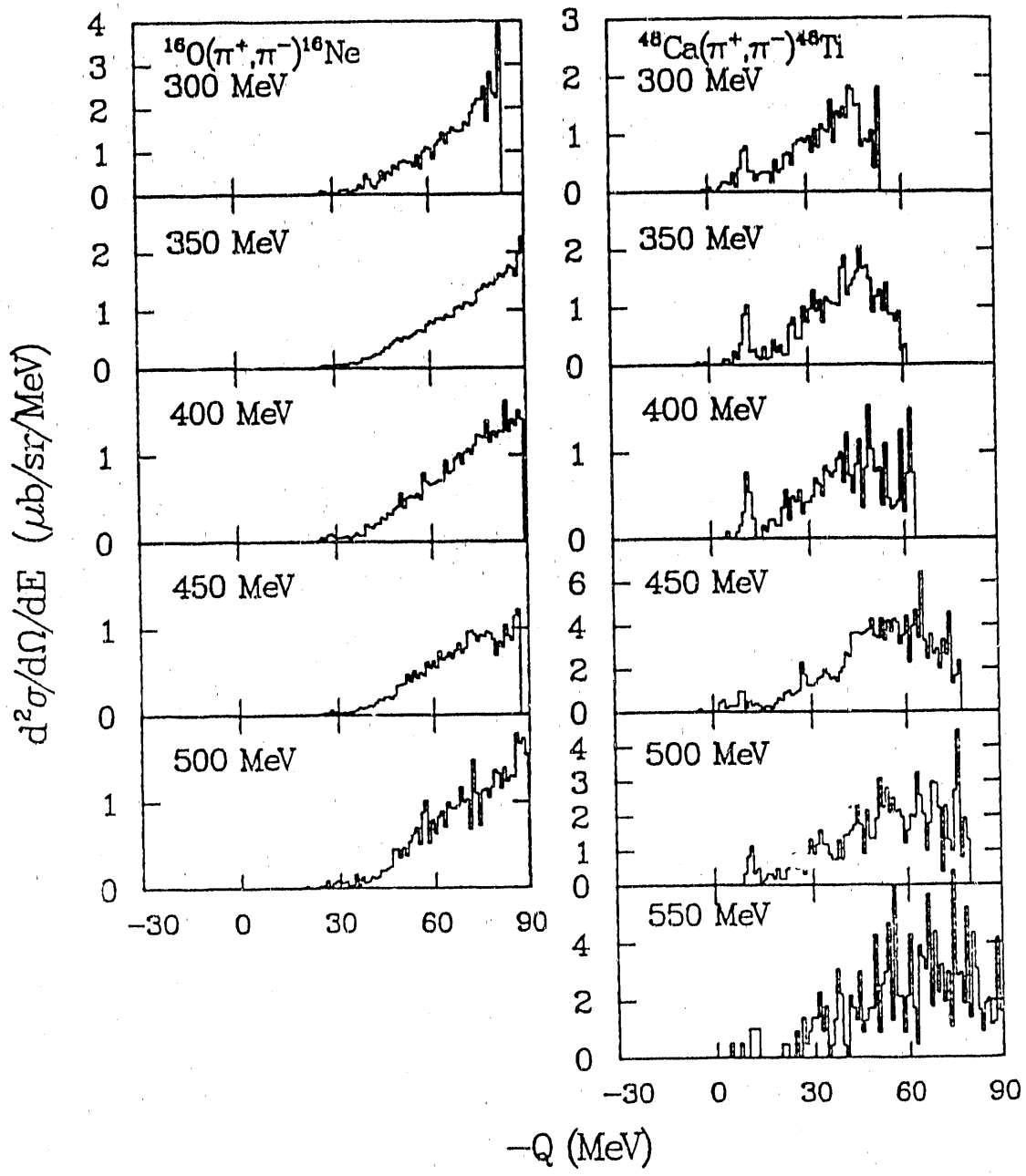

FIG. 13. Spectra for the (π^+,π^-) reaction on ^{16}O and ^{48}Ca at a 5^0 laboratory angle.

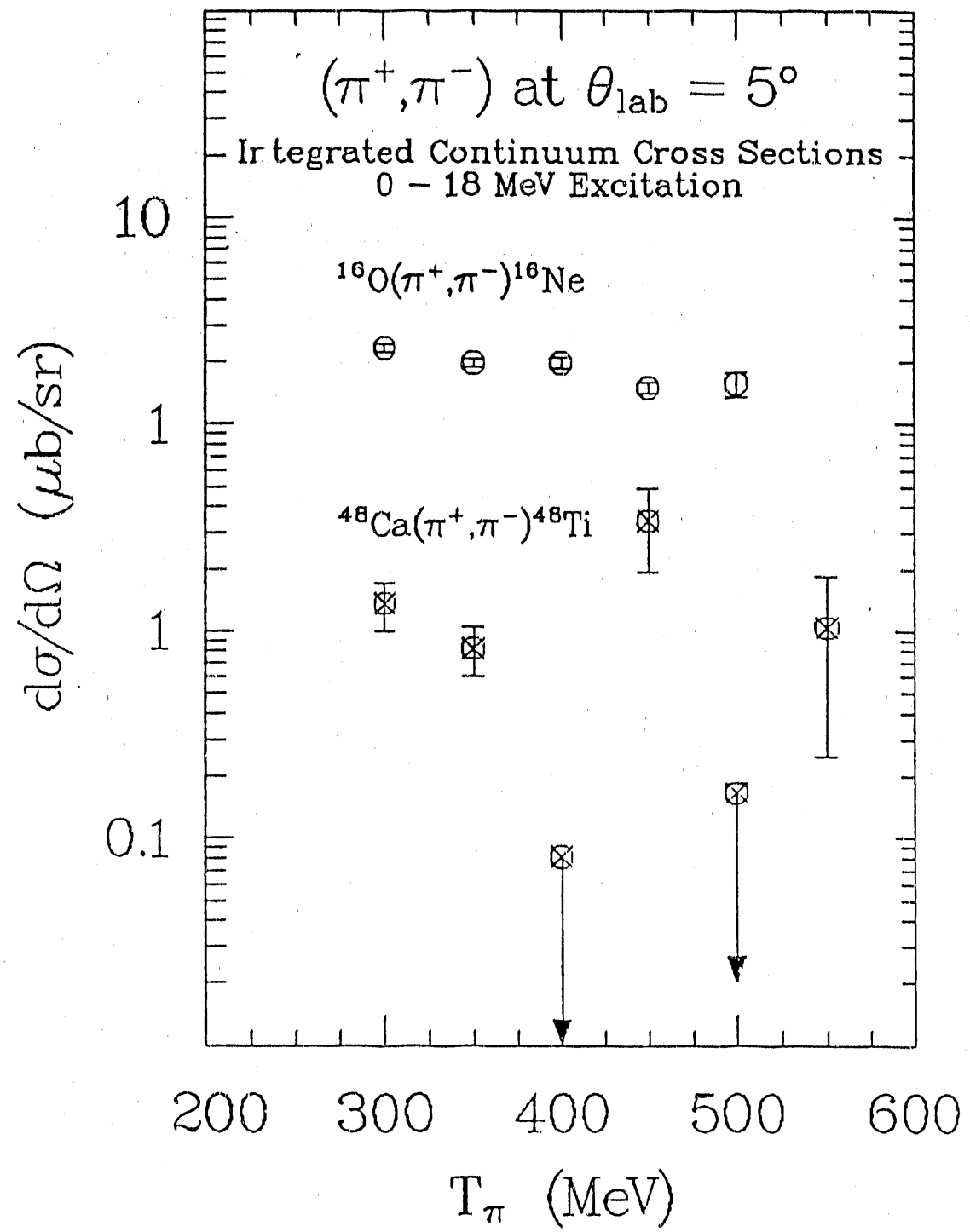

FIG. 14. Integrated nonanalog portions of the spectra of Fig. 13 over 0-18 MeV, as a function of pion beam energy.

by $A^{-7/3}$. The excitation function for ^{14}C is inconsistent with the prediction of a six-quark bag model and with the prediction of a first-order optical model with no free parameters that gives a good representation of the zero-degree SCX excitation function at these energies. One angular distribution has been measured, but there are no published calculations to compare it with.

Measurements have beem made of small-angle differential cross sections on $^{42,44,48}Ca$ over 300-500 MeV and on $^{46,50}Ti$, ^{52}Cr, and ^{54}Fe at 450 MeV. These have been compared with a two-amplitude model, with one amplitude (A) corresponding to transitions through nonanalog states and one (B) arising from short-range correlations which correponds to transitions through nonanalog states. Fits of the calcium analog-state data give a ratio of $|A|/|B|$ that is increasing with energy, as predicted. The ground-state cross sections predicted by this fit are consistently larger than the experimental cross sections by several standard deviations, however. When the other data are compared with the calcium results, the ^{50}Ti and ^{52}Cr cross sections are found to be consistent, but the cross sections for the isospin-one nuclei ^{46}Ti and ^{54}Fe are not, and again the experimental ground-state cross sections are considerably lower than predicted.

Very little data for nonanalog transitions have been measured as yet. The small-angle excitation function for ^{16}O appears flat, but there are no theoretical predictions of its behavior. The nonanalog continuum near threshold is observed to fall with energy, causing peaks to be more prominent. Insufficient data exist to indicate an A-dependence, and no angular distributions have been measured.

References

[1] D. Ernst, Proceedings of the *Conference on Pion-Nucleus Physics: Future Directions and New Facilities at LAMPF*, Los Alamos, 1988 (AIP Conference Proceedings No. 163; Am. Inst. of Phys., New York (1988), p. 513).

[2] D. J. Ernst, J. T. Londergan, G. A. Miller, and R. M. Thaler, Phys. Rev. C *16*, 537 (1977).

[3] LAMPF Experiment No. 1106 (K. S. Dhuga and J. A. McGill, Spokesmen).

[4] D. Ashery, *et al*, Phys. Rev. C *23*, 2173 (1981).

[5] M. Leitch, presented at the *Workshop on Nuclear Structure with Medium Energy Probes*, Santa Fe, New Mexico, 1988 (Bull. Am. Phys. Soc. *33*, 1548 (1988)).

[6] A. L. Williams, *et al*, Phys. Lett. *B216*, 11 (1989).

[7] A compliation of DCX data is found in the Ph.D. dissertation of R. Gilman, University of Pennsylvania (1985), Los Alamos National Laboratory Report no. LA-10524-T, unpublished.

[8] S. H. Rokni, *et al.*, Phys. Lett. *B202*, 35 (1988).

[9] G. E. Parnell, Ph.D. dissertation, Texas A & M University (1987), unpublished; D. J. Ernst and G. E. Parnell, private communication (1988).

[10] G. A. Miller, Phys. Rev. C *35*, 377 (1987).

[11] R. Gilman, *et al*, Phys. Rev. C *35*, 1334 (1987).

[12] N. Auerbach, W. R. Gibbs, and E. Piasetzky, Phys. Rev. Lett. *59*, 1076 (1987).

[13] N. Auerbach, W. R. Gibbs, J. N. Ginocchio, and W. B. Kaufmann, Phys. Rev. C *38*, 1277 (1988).

[14] W. R. Gibbs, private communication.

[15] C. L. Morris, *et al*, Phys. Rev. Lett. *54*, 775 (1985).

END

DATE FILMED

10/25/90